I. The peel test consists of cutting through the polymer overlayer on the electrode to produce a grid of polypyrrole squares. Clear adhesive tape[16] is then applied and smoothed to remove any air bubbles; the tape is then peeled off the surface. For the electrodes functionalized with I we observe no obvious removal of the polypyrrole, whereas when I is not used as a "primer", the polypyrrole either peels spontaneously upon attempting to cut through the polymer (see electrode second from left on the bottom) or is efficiently removed by the adhesive tape. The peel test was done by removing the tape both rapidly and slowly with the same results for electrodes functionalized first with I: no gross removal of polypyrrole is observed.

Treatment of n-type Si with I followed by the formation of polypyrrole improves the durability of the electrode in aqueous electrolytes when it is used as a photoanode for the oxidation of I^- or Fe^{2+}(aq) compared to the durability of electrodes functionalized only with polypyrrole. Conditions, current density, and electrolytes are similar to those reported earlier.[2-5] For example, in one experiment an n-type Si/I/polypyrrole photoanode at +0.41 V vs. SCE in 0.15 M $FeCl_3$/0.5 M $FeCl_2$/1 M HCl gave an initial photocurrent of 7.6 mA/cm^2 that remained constant, or slightly greater, for 25 h. In a parallel experiment with an n-type Si/polypyrrole photoanode, having nearly the same amount of polypyrrole on the surface, photocurrent declined from 6.5 to 1.8 mA/cm^2 in less than 18 h. We attribute the improvement in durability to less H_2O/electrolyte undermining of the polymer when it is covalently anchored to the surface. Detailed studies of durability will be reported in a full paper.

Acknowledgment. We thank the U.S. Department of Energy, Office of Basic Energy Sciences, Division of Chemical Sciences, for support of this research. We thank R. N. Dominey for assistance with the FTIR studies and J. A. Bruce for assistance with the Auger spectroscopy.

Registry No. I, 80906-67-8; pyrrole, 109-97-7; 1-bromo-3-trimethoxysilylpropane, 51826-90-5.

---

(16) Scotch (3M) Brand 810 Magic Transparent Tape (part no. 021200-07378) was used for all peel tests.

Pyridine Coordination Chemistry of Nickel and Platinum Surfaces

Ronald M. Wexler, Min-Chi Tsai, C. M. Friend, and
E. L. Muetterties*

Materials and Molecular Research Division
Lawrence Berkeley Laboratory
and Department of Chemistry, University of California
Berkeley, California 94720

Received November 6, 1981

Pyridine–transition-metal coordination chemistry for molecular species is largely characterized by a conventional σ-donor and π-acceptor interaction of the nitrogen atom with the metal atom.[1] However, in zerovalent or low-valent, coordinately unsaturated mononuclear[2a] and cluster[2b] complexes, there is a potential for subsequent interactions, **1**, whereby a chelating α-pyridyl or a bridging α-pyridyl complex may form. In addition, there are several isolated examples[3] of π-$C_5H_5NML_3$ complexes, **2**, in which pyridine or a substituted pyridine is an η^6-ligand for a metal atom in a low oxidation state. Pyridine coordination chemistry at metal surfaces has been studied by spectroscopic[4] and diffraction[5] techniques, but the available data do not allow unqualified structural interpretations. We present here results of an ultrahigh-vacuum study[6] of pyridine chemistry on various crystal planes of nickel and platinum. Through isotopic labeling studies, an important interaction via α-pyridyl bonding has been incisively established for some specific crystal planes. These data provide a fundamental understanding of a catalytic reaction, namely H–D exchange processes, observed[10] for pyridine and deuterium with metallic catalysts.

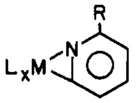

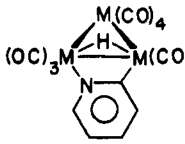

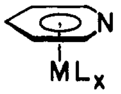

Pyridine adsorbed on the nickel(100) surface at 25 °C, and approximately monolayer[11] coverage exhibited partial (~50%)[12a]

---

(1) Pyridine is a medium-strength field ligand. It lies between ammonia and ethylene in the ligand spectrochemical series.

(2) (a) Cp_2TiR (R = alkyl) reacts with substituted pyridines to give chelating α-pyridyl complexes: Klei, E.; Teuben, J. H. *J. Organomet. Chem.* **1981**, *214*, 53. (b) $Os_3(CO)_{12}$ reacts with pyridine to give $Os_3(CO)_{11}NC_5H_5$. By thermal activation and with further reaction with pyridine, the following transformations have been observed: $Os_3(CO)_{11}NC_5H_5 \xrightarrow{\Delta} HOs_3(\mu_2\text{-}\eta^2\text{-}NC_5H_4)(CO)_{10}$ $(+NC_5H_5) \rightleftharpoons HOs_3(\mu_2\text{-}\eta^2\text{-}NC_5H_4)(CO)_9(NC_5H_5) \rightleftharpoons H_2Os_3(\mu_2\text{-}\eta^2\text{-}NC_5H_4)_{22}(CO)_8 \rightarrow Os_2(\mu_2\text{-}\eta^2\text{-}NC_5H_4)_2(CO)_6$ (Yin, C. C.; Deeming, A. *J. Chem. Soc., Dalton Trans.* **1975**, 2091.

(3) Timms, P. L. *Angew. Chem.* **1975**, *87*, 295; Timms, P. L. *Angew. Chem., Int. Ed. Engl.* **1975**, *14*, 273. Simons, L. H.; Riley, P. E.; Davis, R. E.; Lagowski, J. J. *J. Am. Chem. Soc.* **1976**, *98*, 1044. Riley, P. E.; Davis, R. E. *Inorg. Chem.* **1976**, *15*, 2735. Biederman, H.-G.; Öfele, K.; Tajtelbaum, J. *Z. Naturforsch., A* **1976**, *31B*, 321. Biederman, H.-G.; Öfele, K.; Schuhbauer, N.; Tajtelbaum, J. *Angew. Chem., Int. Ed. Engl.* **1975**, *14*, 639.

(4) (a) Kishi and Ikeda examined the ultraviolet spectra of pyridine chemisorbed on titanium, iron, and nickel films and considered two possible modes of bonding: (i) bonding solely through the nitrogen atom and (ii) bonding through the nitrogen atom and through the aromatic system (Kishi, K.; Ikeda, S. *J. Phys. Chem.* **1969**, *73*, 2559). (b) Kishi et al. in a later study of pyridine chemisorption on nickel and iron films decided that the earlier film studies related to partially oxidized metal film surfaces. They examined the X-ray photoelectron spectra of pyridine on nickel and iron films at 10^{-6}–10^{-8} torr and proposed binding of the pyridine to the unoxidized surfaces through the aromatic system of the pyridine (Kishi, K.; Chinomi, K.; Inoue, Y.; Ikeda, S. *J. Catal.* **1979**, *60*, 228). (c) Morrow et al. from an infrared study of pyridine chemisorbed on silica-supported metals proposed α-pyridyl bonding for Pt, Ir, Os, Rh, and Ru. For nickel, simple bonding only through the nitrogen atom of pyridine was proposed: Morrow, B. A.; Cody, I. A.; Moran, L. E.; Palepu, R. *J. Catal.* **1976**, *44*, 467. (d) Very weak bonding of pyridine to Ag(110) and polycrystalline Ag has been established: Kelemen, S.; Kaldor, A. *Chem. Phys. Lett.* **1980**, *73*, 205. Eesley, G. L. *Phys. Lett. A* **1981**, *81A*, 193. Eesley, G. L.; Simon, D. L. *J. Vac. Sci. Technol.* **1981**, *18*, 629. (e) Demuth et al. studied pyridine chemisorbed on Ag(111) by high-resolution electron energy loss and UV photoemission spectroscopy and proposed a state with a slight tipping of the C_5N ring to bring the N atom close to the surface plane and then at higher coverages a more weakly bound state with primarily metal–nitrogen bonding: Demuth, J. E.; Christman, K.; Sanda, P. N. *Chem. Phys. Lett.* **1980**, *76*, 201.

(5) Gland and Somorjai reported that pyridine forms poorly ordered structures on Pt(111) and Pt(100). On the basis of work-function studies, they proposed bonding of the pyridine through the nitrogen atom: Gland, J. L.; Somorjai, G. A. *Surf. Sci.* **1973**, *38*, 157. *Adv. Colloid Interface Sci.* **1976**, *5*, 205.

(6) For the experimental strategy, experimental procedure, and cleaning procedures, see ref 7, 8, and 9, respectively.

(7) Muetterties, E. L. *Angew. Chem.* **1978**, *90*, 577; *Angew. Chem., Int. Ed. Engl.* **1978**, *17*, 545.

(8) Friend, C. M.; Muetterties, E. L. *J. Am. Chem. Soc.* **1981**, *103*, 767, 773.

(9) Friend, C. M.; Gavin, R. M.; Muetterties, E. L.; Tsai, M.-C. *J. Am. Chem. Soc.* **1980**, *102*, 1717.

(10) Moyes and Wells studied the exchange reaction between D_2 and pyridine over Mn, Co, Ni and W films and over powdered iridium and platinum (Moyes, R. B.; Wells, P. B. *J. Catal.* **1971**, *21*, 86). Selectivity to exchange at the 2 and 6 position of the pyridine ring was observed with nickel (at 42 °C), by far the most selective catalyst.

0002-7863/82/1504-2034\$01.25/0 © 1982 American Chemical Society

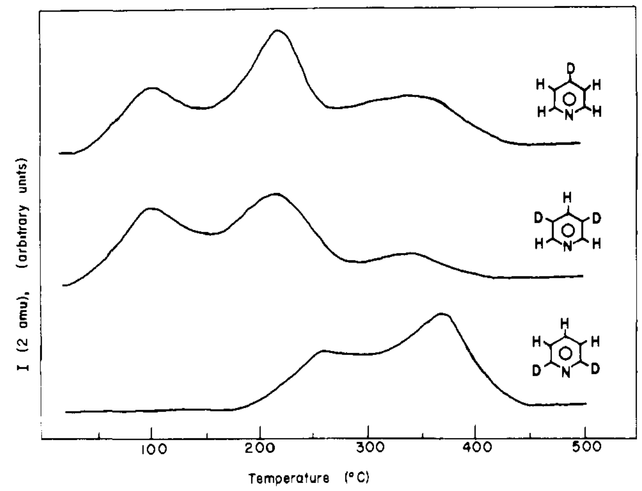

Figure 1. Thermal desorption spectra for H_2 derived from the thermal decomposition of pyridines adsorbed at 25 °C on Ni(100). The heating rates were 20 °C s^{-1} and the coverage[11] was ~1.0.

thermal reversibility[12b] in pyridine chemisorption. Competitive with thermal desorption was thermal decomposition as evidenced by molecular hydrogen (H_2) desorption from the surface. Thermal decomposition of pyridine was distinguished by three overlapping hydrogen desorption peaks of relative intensities of approximately 1:2:2 (the presence of small amounts of carbon or sulfur impurities did not qualitatively alter the character of the pyridine surface chemistry). Similar behavior was observed for pyridine adsorbed on Pt(111), Pt[6(111 × (111)], and Pt(100). These initial data suggested that carbon-hydrogen bond scission occurred regiospecifically. Furthermore, the most plausible chemisorbed species generated in the first C-H bond-breaking process, with assumption of regiospecificity, would be α-pyridyl because this species has substantial precedent in coordination chemistry (vide infra). So that this possibility could be tested, 2,6-$C_5H_3D_2N$, 3,5-$C_5H_3D_2N$, and 4-C_5H_4DN[13] were prepared, and their surface chemistry was studied. These studies provided a relatively comprehensive characterization of the pyridine chemistry on Ni(100). The pyridine thermal decomposition process on this surface is discussed first.

Thermal decomposition of pyridine-*2,6-d_2* on Ni(100) established that *no* H_2 was present in the low-temperature hydrogen desorption peak—only D_2 and small amounts of HD[14] were detected. Complementarily, *no* D_2 or HD appeared in the low-temperature hydrogen peak for either Ni(100)–3,5-$NC_5H_3D_2$ or Ni(100)–4-NC_5H_4D. These results are illustrated partially in Figure 1, which presents the H_2 desorption (decomposition) spectra for the Ni(100) adsorption states of the three labeled pyridine molecules (see Supplementary Material for complete spectral details). These data establish that all[15] pyridine decomposition that occurs on Ni(100) at low temperatures (below ~150 °C) proceeds through an α-pyridyl intermediate.

Table I. Reaction of Ni(100)-Pyridine with D_2 and H_2

starting pyridine	hydrogen added	pyridines formed[a]
2,6-$C_5H_3D_2N$	H_2	pyridine-d_0, -d_1, and -d_2
	D_2	pyridine-d_2 only
3,5-$C_5H_3D_2N$	H_2	pyridine-d_2 only
	D_2	pyridine-d_2, -d_3, and -d_4
4-C_5H_4DN	H_2	pyridine-d_1 only
	D_2	pyridine-d_1, -d_2, and -d_3

[a] In the thermal desorption experiment.

An α-pyridyl species is also a precursor state to adsorbed pyridine that thermally desorbs from Ni(100)—as established by hydrogen–deuterium exchange reactions: the pyridine thermal desorption spectrum for a state(s) generated by reaction of Ni(100)–NC_5H_5 with 10^{-5} torr of D_2 at 80 °C for 5 min[16,17] consisted only of C_5H_5N, C_5H_4DN, and $C_5H_3D_2N$ molecules.[12b,18] To establish the stereochemistry of this reversible C–H bond-breaking process, all three deuteropyridines were subjected to the above type of surface experiment with both H_2 and D_2. Net deuterium exchange was observed only for the two pyridine molecules with no α-deuterium substituents, and net hydrogen exchange was observed only for pyridine-*2,6-d_2* (Table I). All *reversible* C–H bond breaking was regiospecific—it occurred only at α-CH positions. All these data can be described by a pyridine $\rightleftharpoons$ α pyridyl interconversion. These experiments show the reversibility of α-pyridyl formation at temperatures as low as 80 °C. Formation of α-pyridyl surface species occurs at lower temperatures, temperatures that could be as low as 0–20 °C.

Cochemisorption of NC_5H_5 and NC_5D_5 (6:5 molar ratio) to monolayer coverage on Ni(100) at 25 °C followed by thermal desorption led to pyridine desorption over the temperature range of 50 to ~270 °C (the breadth of the pyridine desorption spectrum reflects not simply the molecular pyridine desorption process but conversion of α-pyridyl surface species to molecular pyridine followed by desorption). The molecular composition of the desorbed pyridines included all possible $NC_5H_xD_{5-x}$ molecules.[19] The extent of H–D interchange was a sensitive function of initial, total pyridine coverage.[20]

We can summarize all the observed low-temperature Ni(100) pyridine chemistry with Scheme I; nevertheless, the surface chemistry could be much more complex—there could be states intermediate to pyridine decomposition other than η^2-α-pyridyl species, states such as η^1-α-pyridyl could give rise to singly exchanged (H–D) desorbed pyridines, there could be "molecular" η^6-NC_5H_5 states, etc.[21,22] Our observations can be extended to

---

[11] Coverage is defined as the ratio of surface carbon atoms to surface metal atoms.

[12] (a) This estimate of reversibility is based on Auger electron spectroscopic studies in which the C/Ni and N/Ni ratios were measured after chemisorption of pyridine and then after the thermal desorption experiment. The C/N ratio determined after thermal desorption was slightly lower than before the desorption experiment but the decrease was not considered to be significant. We have no data that provide information about attenuation effects that might alter the ratios. In any case, the estimate of reversibility has a relatively high degree of uncertainty associated with it. The estimate applies only to experiments in which the chemisorption was effected at ~25 °C and in which the heating rate was 20 °C s^{-1}. Alterations in the initial chemisorption temperature and in heating rate should change the degree of thermal reversiblity. (b) At high coverages, the pyridine desorption had two distinct features. The pyridine began to desorb at about 50 °C and the rate of desorption reached a plateau at about 100 °C. The desorption rate remained fairly constant until about 190 °C. The second feature was a sharp peak with a maximum rate at 235 °C with a peak intensity about 50% higher than that of the plateau. Approximately half of the adsorbed pyridine desorbed, based on an analysis of the ratio of nitrogen on the surface to nickel before and after the thermal desorption experiment. At low coverage, the desorption began at about 100 °C and the peak at 235 °C was not observed. Again, about half of the adsorbed pyridine desorbed.

[13] (a) The labeled pyridines were prepared by a slight modification of the method of Bak, et al.[13b] (b) Bak, B.; Hansen, L.; Rastrup-Anderson, J. *J. Chem. Phys.* **1954**, *22*, 2013 (see Supplementary Material).

[14] The small amount of HD observed was presumably due to background hydrogen in the system.

[15] Possibly, *all* pyridine decomposition proceeds through the α-pyridyl intermediate but on the basis of our data, we cannot rule out the possibility that some pyridine decomposition occurs *only* within the higher temperature range and does not proceed through an α-pyridyl intermediate.

[16] A flow system was used in which the ion pumps were closed and the chamber was open to a diffusion pump during the D_2 exposure.

[17] Evacuation to 9 × 10^{-10} torr required about 5 min after the flow of D_2 was stopped.

[18] The observed intensities were corrected for ^{13}C and ^{15}N contributions from the various parent mass ions and for fragment ions.

[19] The relative amounts of masses 79:80:81:82:83:84 at monolayer coverage were roughly 6:3:1:1:3:6.

[20] Only singly exchanged pyridines were detected in addition to unexchanged pyridines when the initial coverages were 0.5 of a monolayer. At low coverages of about 0.15, little interchange was observed; under these conditions, the thermodynamic activity of the H and D chemisorbed atoms (derived from the respective pyridines) was too low to effect a reconversion of an α-pyridyl species to chemisorbed pyridine. Hence, at atmospheric pressure, the extent of reversible desorption and of H–D exchange should be high as is observed for D_2–C_5H_5N with conventional forms of nickel catalysts.

Scheme I

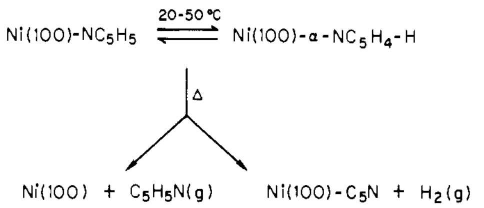

explain the uniquely high regiospecificity of nickel catalysts and the general features of the catalytic studies of Moyes and Wells[10] with full consistency of mechanistic interpretation. We cannot mechanistically interpret the higher temperature decomposition processes for adsorbed pyridines because of possible kinetic isotope effects and because two or more processes may be operative.

The pyridine chemistry of the (100), (111), and 6(111) × (111) surfaces of platinum was similar to that of Ni(100) except that reversible C–H bond breaking (i.e., H–D exchange) was not detected. Other nickel surfaces like Ni(111) and Ni[9(111) × (111)] showed only single broad $H_2(D_2)$ decomposition spectra and no evidence of H–D exchange between C_5H_5N and C_5D_5N. The unique features of Ni(100) may be due to a geometric factor,[26] but further studies with other surfaces are required before this tentative proposal can be seriously advanced. Presently, the conceptual features of this experimental study are being applied to thiophene and furan surface chemistry.

Acknowledgment. This work was supported by the National Science Foundation under Grant Number CHE 8000038. We are also indebted to the Fannie and John Hertz Foundation for a fellowship (R.M.W.) and to the Miller Institute for Basic Research in Science for a grant in the form of a Miller Professorship (E.L.M.).

Registry No. Pyridine, 110-86-1; Ni, 7440-02-0; Pt, 7440-06-4.

Supplementary Material Available: Figures of complete thermal desorption and thermal decomposition spectra for C_5H_5N, 2,6-$C_5H_3D_2N$, 3,5-$C_5H_3D_2N$, and 4-C_5H_4DN adsorption states on Ni(100) (Figures 2–6), experimental procedures for the synthesis of the deuterium-labeled pyridines, and thermal desorption data for 4-$CH_3C_5H_4N$ (8 pages). Ordering information is given on any current masthead page.

---

(21) We present here no spectroscopic data that provide direct information about the structure and stereochemistry of chemisorbed molecular pyridine. A planar C_5H_5N molecule bound in a π (η^3) fashion is a possible chemisorbed state. An η^6 form by its nature would have a stereochemistry (all hydrogen atoms at the same, relatively large distance from surface metal atoms) that would not necessarily lead to regiospecific C–H bond scission at elevated temperatures. In contrast, a molecular state in which pyridine is bound largely through the nitrogen atom (σ-donor and π-acceptor interactions with the ring plane either normal to the surface or slightly tipped) could, through a rocking mode, bring either of the two α-CH hydrogen atoms close to the surface atoms—a stereochemistry that seems to invariably[23-25] lead to C–H bond scission on these metal surfaces. We favor the latter form for Ni(100)–N-C_5H_5.

(22) The coordination chemistry of 4-methylpyridine on Ni(100) was essentially identical with that of pyridine (see Supplementary Material). This fact is supportive of our characterization of the molecular pyridine chemisorption state. Were pyridine bonded as an η^6 ligand in a plane parallel to the surface plane, the methyl substituent in 4-methylpyridine should significantly perturb the surface chemistry of the substituted pyridine as in the qualitative difference between benzene and toluene surface chemistry on nickel reported by Friend and Muetterties.[8]

(23) Muetterties, E. L. *ACS Symp. Ser.* **1981**, *155*, 273.

(24) Gavin, R. M.; Reutt, J.; Muetterties, E. L. *Proc. Natl. Acad. Sci. U.S.A.* **1981**, *78*, 3981.

(25) Muetterties, E. L. *Proc. Int. Conf. Organomet. Chem. 10th* **1981**, August. Muetterties, E. L. *Pure Appl. Chem.* **1982**, *54*, 83.

(26) The diagonal distance of the nickel(100) unit cell is nearly ideal for the conversion of a chemisorbed pyridine molecule, initially bound through the nitrogen atom at a single metal atom, to a μ-η^2-α-pyridyl state. This diagonal separation is structurally optimal for an α-pyridyl species. The distances used for Ni–N and Ni–C interactions for an α-pyridyl complex were 1.91 and 1.85 Å, respectively.

Orbital Rotation in the Lowest Triplet State of Benzophenone

K.-P. Dinse

Max-Planck-Institut für Medizinische Forschung
D-6900 Heidelberg, West Germany

D. W. Pratt*

Department of Chemistry, University of Pittsburgh
Pittsburgh, Pennsylvania 15260

Received November 9, 1981

An orbital is a mathematical function, a solution of the wave equation describing a bound state of a single electron. We also use this term to refer to eigenfunctions of the Hartree–Fock effective Hamiltonian, as in the SCF LCAO–MO approximation for many-electron systems. The atomic orbitals we use in this approach have no objective significance. However, they are convenient "building blocks" for constructing approximate molecular orbitals because they allow us to visualize the electron density in the molecule by breaking it down into the more familiar contributions of each of its component parts. Thus, when we speak of an "$n\pi^*$" state[1] of benzophenone, we are clearly referring to an excited state derived from a single configuration in which an electron is promoted from the oxygen 2p-type "lone-pair" orbital to an antibonding π^* orbital. The currently accepted view is that this is, in fact, an accurate description of the lowest excited states of many aromatic carbonyls, including triplet benzophenone.[2] However, recent experimental results on this prototype system,[3] summarized herein, suggest that this is not the case and further reveal new properties of such excited states which may be of chemical importance.

Our experiments were performed on a single crystal of 4,4′-dibromodiphenyl ether (DDE) containing ~0.1 mol % of an enriched perdeuterio[^{17}O]benzophenone (^{17}O-BP-d_{10}) guest, which was immersed in pumped liquid helium at 1.2 K, excited with a filtered Hg arc, and examined by optically detected magnetic resonance (ODMR) and electron–nuclear double resonance (ODENDOR) spectroscopy at both zero and high magnetic fields (zf and hf).[4] In contrast to the behavior of ^{16,18}O-BP-h_{10} or -d_{10}, each of the electron spin transitions in the zf ODMR spectrum of ^{17}O-BP-d_{10} is split into several components by the combined effect of the ^{17}O ($I = {}^5/_2$) quadrupole and second-order hyperfine interactions. Direct measurements of the nuclear sublevel splittings in each of the three electron spin manifolds were made with an accuracy of ≤400 kHz by the zf ODENDOR technique. Figure 1 shows some representative spectra obtained for the T_z–T_y transition. First-order ^{17}O hyperfine splittings were observed in the hf ODMR experiments; in this case, the presence of a well-defined quantization axis made possible measurements of these splittings, which vary from 0 to 150 MHz, as a function of the angles between the laboratory field and the crystallographic axes of the host with a precision of ±3 MHz and ±2°. Additional structure in each of the hyperfine components, produced by the ^{17}O nuclear quadrupole and Zeeman interactions, was revealed by hf ODENDOR experiments at selected orientations of the crystal.

A treatment[3] of these data using the full spin Hamiltonian of the $S = 1$, $I = {}^5/_2$ system yields the principal values of the electron fine-structure ($\mathbf{D}'$), oxygen hyperfine ($\mathbf{A}''$), and oxygen quadrupole ($\mathbf{Q}''$) tensors and the relative orientation of their principal axes. Of particular interest are the diagonal forms of the quadrupole

---

(1) R. S. Mulliken, *J. Chem. Phys.* **3**, 564 (1935).

(2) See, for example, N. J. Turro, "Modern Molecular Photochemistry", Benjamin-Cummings, Menlo Park, CA, 1978.

(3) G. Wäckerle, M. Bär, H. Zimmermann, K.-P. Dinse, S. Yamauchi, R. J. Kashmar, and D. W. Pratt, *J. Chem. Phys.*, in press. For preliminary results, see S. Yamauchi and D. W. Pratt, *Chem. Phys. Lett.* **60**, 145 (1978).

(4) For a review, see D. W. Pratt in "Excited States", Vol. 4, E. C. Lim, Ed., Academic Press, New York, p 137.

0002-7863/82/1504-2036$01.25/0